Bulletin of Electrical Engineering and Informatics
Vol. 14, No. 2, April 2025, pp. 845~853
ISSN: 2302-9285, DOI: 10.11591/eei.v14i2.8465

Enhancing solar panel efficiency through dual-axis tracking and fresnel lens concentration: an image processing approach

Muhammad Ghozi Witsqa Ramadhan, Levin Halim, Faisal Wahab
Center of Control, Automation, and Systems Engineering, Department of Electrical Engineering, Faculty of Engineering Technology, Parahyangan Catholic University, Bandung, Indonesia

Article Info

Article history:

Received Mar 14, 2024
Revised Oct 17, 2024
Accepted Nov 19, 2024

Keywords:

Camera
Fresnel lens
Image processing
Solar panel
Solar tracking system

ABSTRACT

Solar energy is currently utilized as an inexhaustible renewable energy source. Solar panels can convert solar energy into electrical energy that humans can use. The drawback of solar panels is that they cannot always be perpendicular to the sun, causing a decrease in the intensity of incoming light. Therefore, in this research, a solar tracking system with a fresnel lens was designed using image processing to increase the output of solar panels. In this research, programming was done using Python software for image processing using the hue, saturation, value (HSV) color, and space model, which was then connected with Arduino using the PyFirmata library to move the motor. In this research, solar panels with a fresnel lens and solar tracking were implemented. Data collection was performed on the output voltage of the solar panel. The research concludes that solar panels with solar tracker and fresnel lens have a higher average output voltage of 7.53 V than passive solar panels with an average output voltage of 6.38 V. Also, the average output voltage increased by 18.02% after implementing the solar tracking system and adding the fresnel lens.

Corresponding Author:

Levin Halim
Center of Control, Automation, and Systems Engineering, Department of Electrical Engineering
Faculty of Engineering Technology, Parahyangan Catholic University
St. Ciumbuleuit 94, Bandung 40141, West Java, Indonesia
Email: halimlevin@unpar.ac.id

1. INTRODUCTION

Massive consumption of fossil fuels at specific points can affect the depletion of these resources [1]. The formation of fossil energy also takes a very long time and requires very high costs in the production process [2]. Therefore, renewable energy, such as solar energy, is necessary as an alternative energy source [3].

One alternative energy source is sunlight, a renewable energy source [4], [5]. Indonesia has long hours of daylight, nearly 12 hours daily, making it the largest solar energy absorber in ASEAN [6], [7]. Solar energy is energy produced by the heat radiated from the sun. One thing that can be utilized from solar energy is an endless source of electricity generation [8], [9].

A solar panel is an electronic device that can convert solar energy into electrical energy [10]. Solar panels consist of an array of solar cells [11]. Solar cells are devices or active elements that can convert light energy into electrical energy using the principle of the photovoltaic effect [12]. Solar panels are generally divided into two main categories: passive and active [13]. Passive solar panels are static or do not involve any electronic equipment to track the sun's position [14]. In contrast, active solar panels are connected to electronic devices to track the sun [15]. Compared to passive panels, active panels are designed to track all positions of the sun, thus approaching the typical geometric point [16]-[18].

With the rapid development of knowledge and technology, various imaging methods are being applied to address everyday problems. The implementation of imaging methods is widely carried out, especially in image processing done by computers, commonly referred to as digital image processing. Digital image processing is a field that studies techniques for processing images and videos digitally using computers [19]. Image processing is also being applied to active solar panels [20]. Initially, the direction of active solar panels was controlled using four light dependent resistors (LDRs) as sensors, and then image processing on solar panels began to be implemented. The addition of cameras and image-based processing methods significantly reduces tracking errors present in LDR sensor-based active solar panels [21]. This image processing requires a library to process images or videos to extract information from the data. Open source computer vision library (OpenCV) is a library developed by intel that focuses on simplifying programs related to digital images [22]. OpenCV is an open-source computer vision library for C/C++ programming languages, and it has also been developed for Python, Java, and MATLAB [23].

In the application of solar panels, the intensity of light on the solar panels is often disturbed due to environmental factors. The light intensity emitted by the sun can be enhanced by utilizing light collectors. fresnel lenses function to focus light or are commonly used as light collectors. There are two types of fresnel lenses: refractive lenses, which function to refract light passing through the lens, and reflective mirrors, which function to reflect light [24], [25].

Therefore, this research will design and implement a device that combines a solar tracking system with a fresnel lens as a concentrator using image processing. The developed solar tracking system is a dual-axis solar tracking system that can move in both horizontal and vertical planes. A fresnel lens is placed directly above the solar panel to increase the intensity of sunlight. Then, the system is tested by comparing the voltage output values of the solar panel before and after using the solar tracking system along with the fresnel lens.

2. METHOD

The design of this solar tracking system consists of a mechanical system, an electrical system, and an image processing algorithm. Figure 1 shows the block diagram of the sun tracking system. The solar tracker design has two axes: rotation (pan) and rotation (tilt). The reference positions of the sun are based on altitude and azimuth. The altitude angle corresponds to the pan, while the azimuth angle corresponds to the tilt. Based on the block diagram, it starts with the camera capturing the sun's position. Then, it proceeds with image processing using Python software with hue, saturation, value (HSV) color model, and sun position detection. Communication between Python and Arduino is established using the PyFirmata library so that Arduino can control servo movements to align with the sun's position. The placement of the camera and solar panel is aligned; therefore, when the camera faces the sun's position, the solar panel also faces the sun's position.

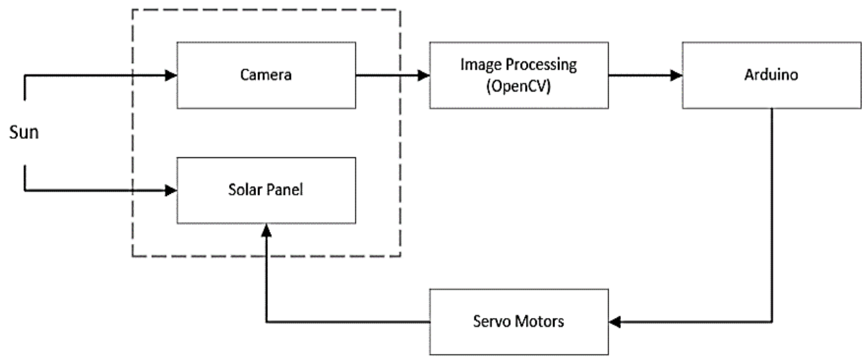

Figure 1. The block diagram of the sun tracking system

2.1. System design

The system has several main components: one solar panel, a USB camera, two servo motors, two Arduino UNOs, and one DC voltage sensor. The designed system is a dual-axis solar tracking system, with the camera positioned at the top of the solar panel for image capture and processing. The two servo motors are used to move the solar panel. The first servo motor is designed to move the solar panel horizontally, and the second is designed vertically. Then, directly above the solar panel, a rectangular-shaped fresnel lens is placed at a calculated distance so that the light refracted by the lens can cover the entire surface of the solar panel. Figure 2 shows an isometric view of the overall design along with dimensions.

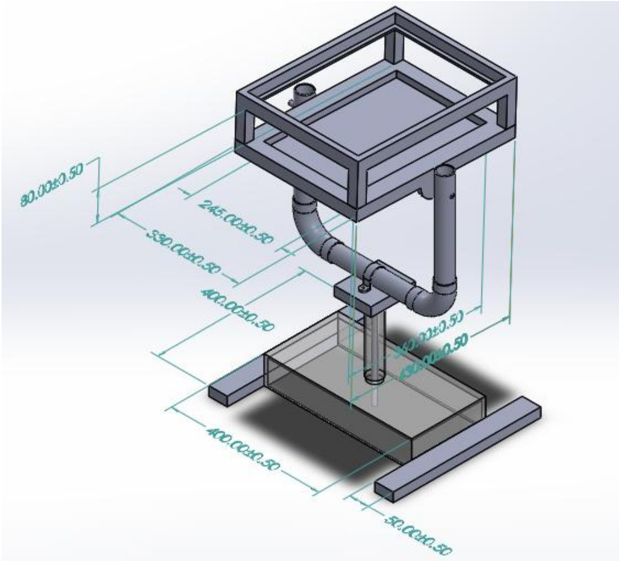

Figure 2. Isometric view of the design along with dimensions (mm)

2.2. System schematic

The system has electrical devices that respond to the solar tracker to move the servo motors. Figure 3 shows the system schematic of the sun tracking system. Based on the information in Figure 3, it is known that both GND pins of the servo are connected to the Arduino's GND, and both VCC pins of the servo are connected to the 5 V source on the Arduino. Then, the signal pin from the pan servo is connected to digital pin 9, while the tilt servo is connected to digital pin 10 on the Arduino.

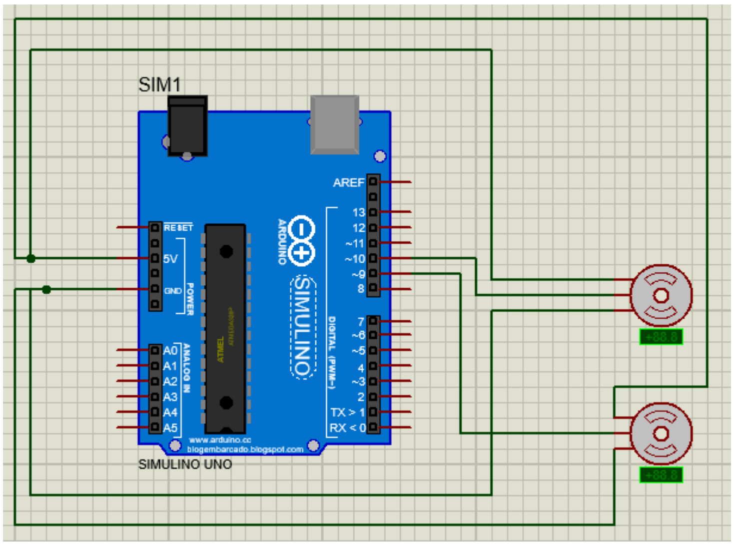

Figure 3. System schematic of the sun tracking system

2.3. Image processing window display

The image processing display with the OpenCV platform using Python is designed to show two windows. The first window will display the camera capture results and the HSV color model settings. Then, the second window will display the masked results after adjusting the HSV color model.

Figure 4(a) shows the image processing window display. The window display can show the camera capture results. At the top of the window, adjustments can be made to HSV values by setting the minimum H, maximum H, minimum S, maximum S, minimum V, and maximum V values. Figure 4(b) shows the masking result based on the camera capture that has been successfully done by adjusting the HSV values.

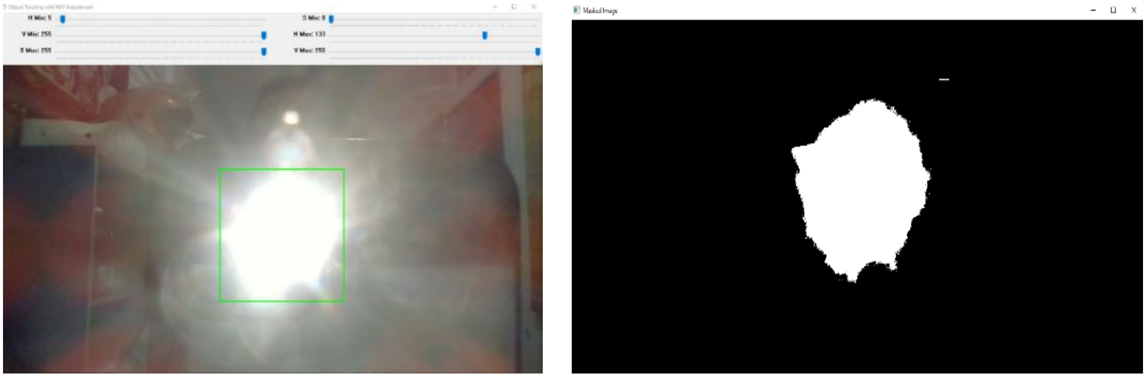

(a) (b)

Figure 4. The image processing window displays: (a) camera capture and (b) masking result

2.3. Solar tracking algorithm

The solar tracking algorithm is initiated by capturing images of the sun object with the help of a camera. Afterward, it proceeds with image processing in Python software. The image processing starts with capturing images from the camera and then adjusting the HSV so that the object can be detected based on the masking result. Then, in the image processing results, a check is made to determine whether the sun's position is in the camera's center. At this stage, sun detection is divided into two axes, x, and y, based on the screen's pixel size displayed from the image processing results. The screen pixels defined in image processing are 640×480. So, the x-axis ranges from 0 to 640, and the y-axis ranges from 0 to 480. Therefore, the center point on the camera can be defined at the coordinate position (x, y). The center point based on the screen pixels is (320,240). Suppose the sun's position is not in the center of the camera. In that case, the image processing will read the contours detected by the camera and then convert the center point of the detected contour into frame coordinates. After that, the frame coordinates of the center point of the contour are converted into servo motor rotation angles. In the frame coordinate, the x-axis ranges from 0 to 640 becomes 0° to 180°, and the y-axis from 0 to 480 becomes 30° to 150°. Then, the converted angle from the center point of the detected contour based on the frame coordinates will be the input angle for the servo motor. Based on Figure 5, the light object has been successfully detected according to the masking result. At that time, the light was not in the center of the frame, so the servo motors moved accordingly to a certain angle, as displayed on the serial monitor on the left side of Figure 5.

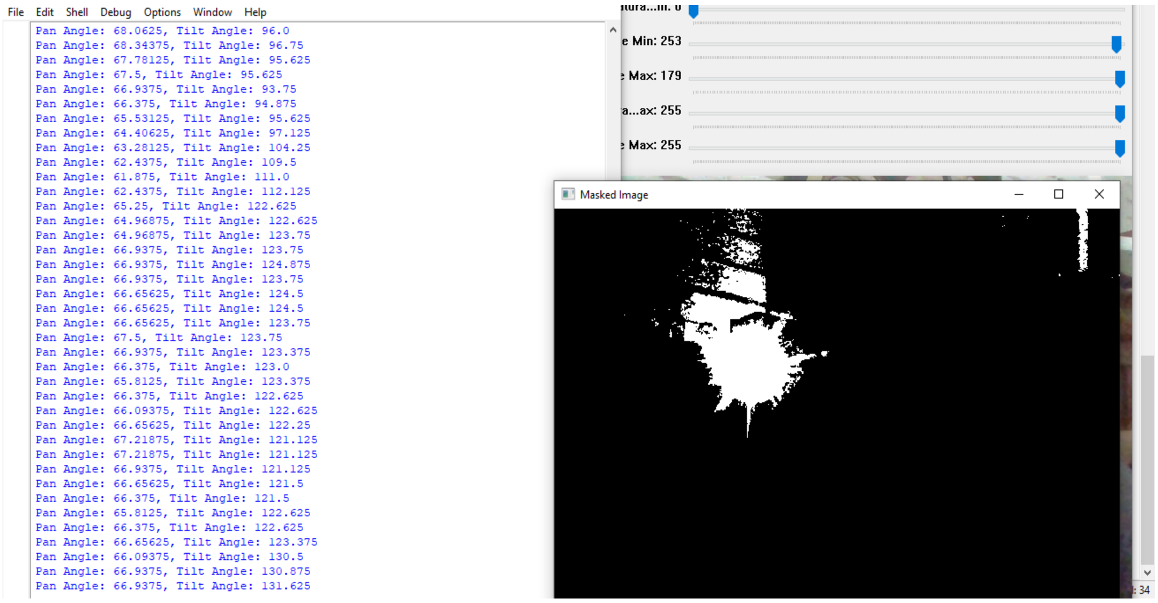

Figure 5. Solar tracking system test

2.4. Calculation of the distance between the fresnel lens and the solar panel

For the refractive lens type of fresnel lens, the refracted light is focused at a specific focal point with a particular focal length. Figure 6 illustrates the required distance for the diffracted light to cover the receiver surface. (x) represents the distance between the fresnel lens and the receiver, with a specific focal length denoted as f. To find the distance between the fresnel lens and the receiver, simple trigonometric functions are used on the flat plane triangle, as the diffracted light by the fresnel lens generally converges at one point and forms a flat plane triangle [26] shown in (1):

$$tanA = \text{tanB} \quad (1)$$

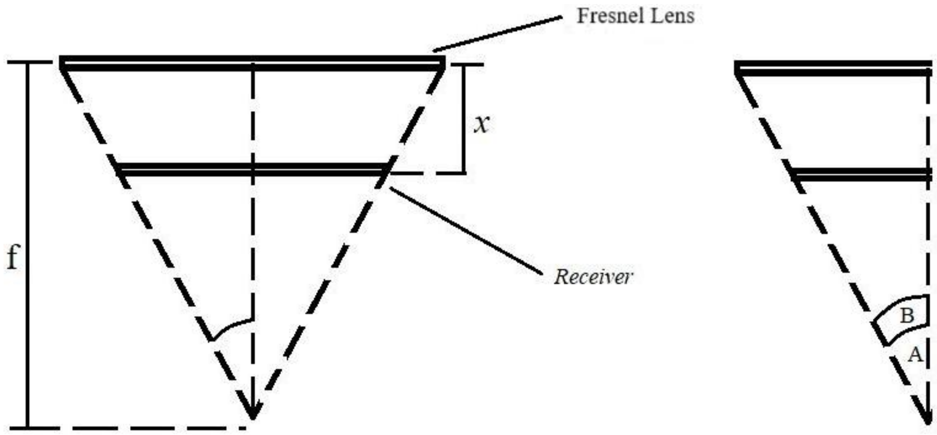

Figure 6. Illustration of calculating the distance between the fresnel lens and the solar panel

2.5. Data acquisition

The data acquisition process was conducted simultaneously on passive solar panels (without tracker and fresnel lens) and active solar panels (with tracker and fresnel lens). The testing lasted 6 hours, starting at 09:00 AM and ending at 03:00 PM. Data collection of the output voltage values from both solar panels was done every 15 minutes. After obtaining the research data, the output voltage data was analyzed and compared in graphs.

3. RESULTS AND DISCUSSION

3.1. Calculation of the distance between the fresnel lens and the solar panel

The chosen fresnel lens for this system is rectangular, with dimensions of 400×300 mm and a focal length of 600 mm, and made of plastic. The choice of fresnel lens is adjusted to the dimensions of the solar panel, which has dimensions of 350×235 mm. In (2) shows that the distance between the fresnel lens and the solar panel is 75 mm or about 80 mm so that the diffracted light can cover the entire surface of the solar panel.

$$tanA = \text{tanB} \quad (2)$$
$$\frac{200}{600} = \frac{175}{600-x}$$
$$x = 600 - 525$$
$$x = 75 \text{ mm}$$

3.2. System realization

The designed system consists of a base-shaped beam at the bottom. Then, there are Y-shaped poles for placing the solar panels and fresnel lenses. Figure 7(a) shows the system realization and implementation. On the other hand, Figure 7(b) shows the part at the bottom of the base, where there is servo motor 1 (pan) to rotate the vertical shaft. Servo motor 1 is connected to a GT2 timing pulley with a bore diameter of 6 mm. On the vertical shaft, there is also a GT2 timing pulley connected with a bore diameter of 10 mm. To enable the vertical shaft to rotate, the servo and the vertical shaft are connected with a 6 mm wide GT2 belt. Figure 7(c) shows the placement of servo motor 2 (tilt) to rotate the horizontal shaft. Servo motor 2 is connected to a

GT2 timing pulley with a bore diameter of 6 mm. On the horizontal shaft, there is also a GT2 timing pulley connected with a bore diameter of 10 mm. To enable the horizontal shaft to rotate, the servo and the horizontal shaft are connected with a 6 mm wide GT2 belt. Figure 8 shows that with a distance of 80mm between the fresnel lens and the solar panel, the light refracted by the fresnel lens can cover the entire surface of the solar panel.

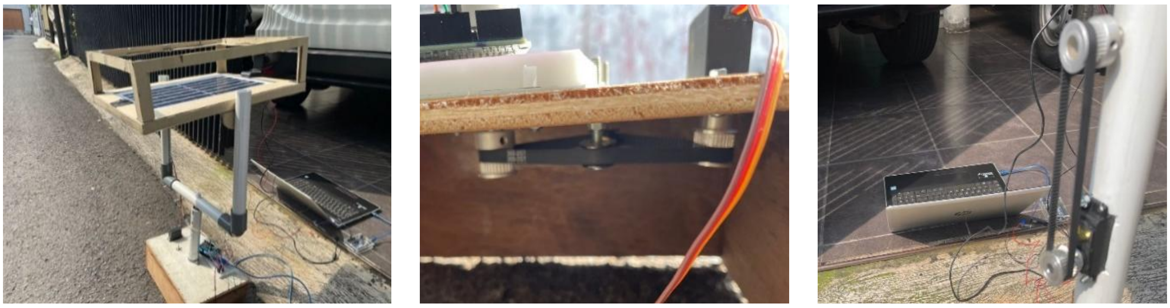

(a) (b) (c)

Figure 7. System implementation: (a) the system that has been created, (b) the vertical shaft motor component, and (c) the horizontal shaft motor component

Figure 8. The distance between the fresnel lens and the solar panel

3.3. Comparison of output voltage between passive solar panel and active solar panel with fresnel lens

After experiments on both solar panels have been conducted simultaneously, a table comparing the output voltage results from both testing conditions of the solar panels is shown in Table 1. Based on Table 1, the position of the solar panel relative to the sun and the level of light intensity entering the solar panel affect the output voltage value of the solar panel. This is shown by the fact that, at the same solar radiation value and time, the solar panel with a solar tracker and fresnel lens has a greater output voltage value than the solar panel without a tracker and a fresnel lens. Based on Table 1, the output voltage value of the passive solar panel reaches its highest point at 12:45 PM, measuring 6.84 V, and its lowest point at 09:45 AM, measuring 5.98 V. The highest output voltage value of the active solar occurs at 2:30 PM, measuring 8.04 V, while the lowest output voltage value occurs at 9:30 AM, measuring 6.89 V. The average output voltage value on the active solar panel is higher than that of the passive solar panel. The average output voltage in the active solar panel is 7.53 V, while in the passive solar panel, it is 6.38 V. This occurs because the light intensity received by the active solar panel is higher than the passive solar panel. If the solar panel always remains perpendicular to the sunlight, the output voltage will also increase. And, of course, it significantly impacts the amount of electrical energy generated daily. A fresnel lens is added to the system in the active solar panel. Thus, the increase in light intensity entering the solar panel can be enhanced using a fresnel lens that concentrates light. Therefore, by combining both of these systems, the output voltage value generated by the active solar panel can increase significantly.

Figure 9 shows a graph comparing the two solar panels. Based on the graph, it can be seen that the solar panel implementing the sun tracker with a fresnel lens has a higher graph compared to the solar panel without the sun tracker and the fresnel lens. According to the results of the experiments on both solar panels, the average output voltage value increased by 18.02% after implementing the solar tracking system and adding the fresnel lens. This is because in the active solar panel, the solar panel's position can always face the sun, and the light intensity is higher due to the light diffracted through the fresnel lens.

Table 1. Comparison of output voltage between passive solar panel and active solar panel with fresnel lens

Time	Output voltage of passive solar panel (V)	Output voltage of active solar panel with fresnel lens (V)
09:00 AM	6.21	7.19
09.15 AM	6.15	6.95
09:30 AM	6.10	6.89
09:45 AM	5.98	6.96
10:00 AM	6.13	7.02
10:15 AM	6.05	7.18
10:30 AM	6.26	7.29
10:45 AM	6.27	7.35
11:00 AM	6.18	7.33
11:15 AM	6.20	7.34
11:30 AM	6.18	7.66
11:45 AM	6.49	7.97
12:00 PM	6.67	7.88
12:15 PM	6.71	7.95
12:30 PM	6.79	7.84
12:45 PM	6.84	8.01
01:00 PM	6.74	7.55
01:15 PM	6.62	7.82
01:30 PM	6.59	7.84
01:45 PM	6.67	7.65
02:00 PM	6.25	7.71
02:15 PM	6.31	7.78
02:30 PM	6.81	8.04
02:45 PM	6.19	7.53
03:00 PM	6.13	7.61

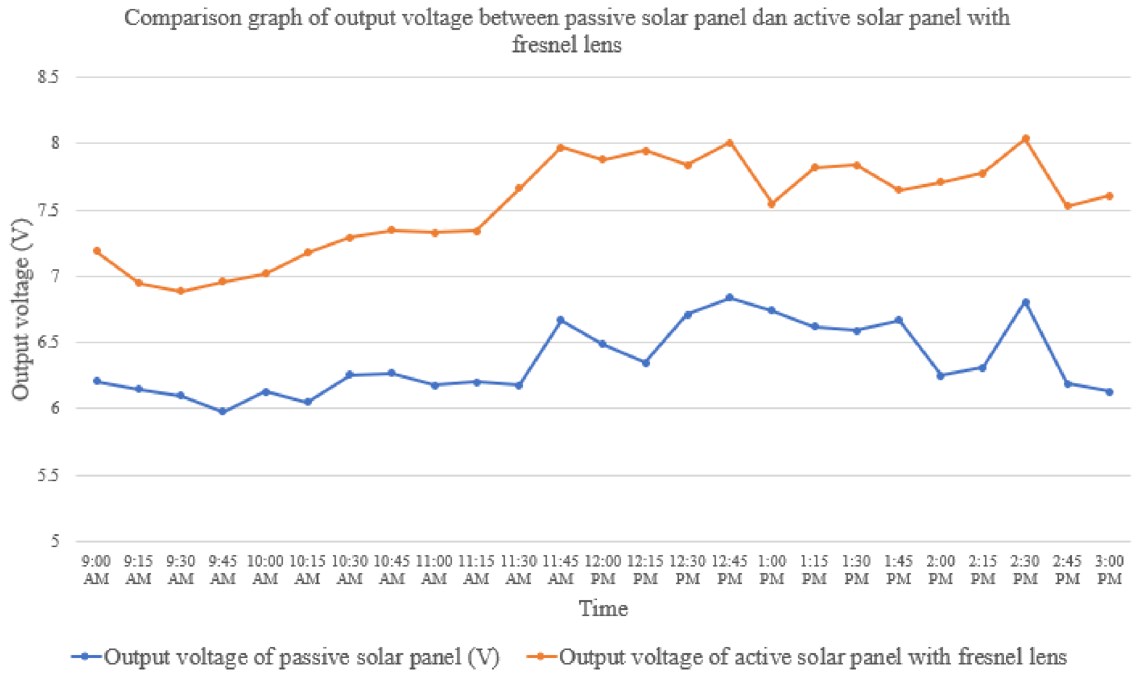

Figure 9. Comparison graph of output voltage between passive solar panel and active solar panel with fresnel lens

4. CONCLUSION

The design results prove that camera image processing has been successfully designed and implemented in the solar tracking system. Applying a fresnel lens to diffract light onto the entire surface of the solar panel requires a distance of about 80 mm. Based on the research, the position of the solar panel relative to the sun and the level of light intensity received by the solar panel affect the output voltage value of the solar panel. This can be proved by the fact that, at the same solar radiation value and time, the solar panel with a solar tracker and fresnel lens has a higher output voltage value than those without. The solar panel with a solar tracker and fresnel lens has a higher average output voltage value, which is 7.53 V, compared to the passive solar panel, which has an average output voltage value of 6.38 V. By implementing a solar tracking system and a fresnel lens, the solar panel can operate at its optimal conditions at all times. This is evidenced by the average output voltage value increasing by 18.02% after implementing the solar tracking system and adding the fresnel lens.

REFERENCES

[1] A. Pareek, R. Dom, J. Gupta, J. Chandran, V. Adepu, and P. H. Borse, "Insights into renewable hydrogen energy: Recent advances and prospects," *Materials Science for Energy Technologies*, vol. 3, pp. 319–327, 2020, doi: 10.1016/j.mset.2019.12.002.

[2] J. L. Holechek, H. M. E. Geli, M. N. Sawalhah, and R. Valdez, "A Global Assessment: Can Renewable Energy Replace Fossil Fuels by 2050?," *Sustainability*, vol. 14, no. 8, pp. 1-22, Apr. 2022, doi: 10.3390/su14084792.

[3] J. Windarta, A. Y. Wardaya, and S. Saptadi, "Solar power plant on the rooftop of the Diponegoro University Rectorate: a technical and economic study," *Bulletin of Electrical Engineering and Informatics*, vol. 12, no. 4, pp. 1936–1946, Aug. 2023, doi: 10.11591/eei.v12i4.3497.

[4] U. H. Salman, S. F. Nawaf, and M. O. Salih, "Studying and analyzing the performance of photovoltaic system by using fuzzy logic controller," *Bulletin of Electrical Engineering and Informatics*, vol. 11, no. 3, pp. 1687–1695, Jun. 2022, doi: 10.11591/eei.v11i3.3680.

[5] A. Qazi *et al.*, "Towards Sustainable Energy: A Systematic Review of Renewable Energy Sources, Technologies, and Public Opinions," *IEEE Access*, vol. 7, pp. 63837–63851, 2019, doi: 10.1109/ACCESS.2019.2906402.

[6] M. A. Budiyanto, Nasruddin, and M. H. Lubis, "Turbidity factor coefficient on the estimation of hourly solar radiation in Depok City, Indonesia," *Energy Reports*, vol. 6, pp. 761–766, Feb. 2020, doi: 10.1016/j.egyr.2019.11.152.

[7] N. A. Handayani and D. Ariyanti, "Potency of Solar Energy Applications in Indonesia," *International Journal of Renewable Energy Development*, vol. 1, no. 2, pp. 33–38, Jul. 2012, doi: 10.14710/ijred.1.2.33-38.

[8] T. Ding and G. W. Ho, "Using the sun to co-generate electricity and freshwater," *Joule*, vol. 5, no. 7, pp. 1639–1641, Jul. 2021, doi: 10.1016/j.joule.2021.06.021.

[9] Q. Zeng *et al.*, "Integrated Photorechargeable Energy Storage System: Next-Generation Power Source Driving the Future," *Advanced Energy Materials*, vol. 10, no. 14, Apr. 2020, doi: 10.1002/aenm.201903930.

[10] N. S. Lewis, "Introduction: Solar Energy Conversion," *Chemical Reviews*, vol. 115, no. 23, pp. 12631–12632, Dec. 2015, doi: 10.1021/acs.chemrev.5b00654.

[11] M. C. Putnam *et al.*, "Si microwire-array solar cells," *Energy and Environmental Science*, vol. 3, no. 8, pp. 1-6, 2010, doi: 10.1039/c0ee00014k.

[12] A. S. Al-Ezzi and M. N. M. Ansari, "Photovoltaic Solar Cells: A Review," *Applied System Innovation*, vol. 5, no. 4, pp. 1-17, Jul. 2022, doi: 10.3390/asi5040067.

[13] A. Maleki, A. Haghighi, M. El H. Assad, I. Mahariq, and M. A. Nazari, "A review on the approaches employed for cooling PV cells," *Solar Energy*, vol. 209, pp. 170–185, Oct. 2020, doi: 10.1016/j.solener.2020.08.083.

[14] A. Awasthi *et al.*, "Review on sun tracking technology in solar PV system," *Energy Reports*, vol. 6, pp. 392–405, Nov. 2020, doi: 10.1016/j.egyr.2020.02.004.

[15] H. Zsiborács, G. Pintér, A. Vincze, and N. H. Baranyai, "A Control Process for Active Solar-Tracking Systems for Photovoltaic Technology and the Circuit Layout Necessary for the Implementation of the Method," *Sensors*, vol. 22, no. 7, pp. 1-20, Mar. 2022, doi: 10.3390/s22072564.

[16] P. Singh, R. Pahuja, M. Karwasra, S. Beniwal, M. Bansal, and A. Dadhich, "Dual Axis Solar Tracking System for Solar Panel," *Bulletin of Electrical Engineering and Informatics*, vol. 5, no. 4, pp. 403–411, Dec. 2016, doi: 10.11591/eei.v5i4.565.

[17] S. K. Venkata and J. S. Rajshekar, "Design and Development of an Automated Multi Axis Solar Tracker Using PLC," *Bulletin of Electrical Engineering and Informatics*, vol. 2, no. 3, pp. 204–211, Sep. 2013, doi: 10.11591/eei.v2i3.205.

[18] G. Li, J. Tang, and R. Tang, "Performance and Design Optimization of a One-Axis Multiple Positions Sun-Tracked V-trough for Photovoltaic Applications," *Energies (Basel)*, vol. 12, no. 6, pp. 1-23, Mar. 2019, doi: 10.3390/en12061141.

[19] S. Ma, X. Zhang, C. Jia, Z. Zhao, S. Wang, and S. Wang, "Image and Video Compression With Neural Networks: A Review," *IEEE Transactions on Circuits and Systems for Video Technology*, vol. 30, no. 6, pp. 1683–1698, Jun. 2020, doi: 10.1109/TCSVT.2019.2910119.

[20] R. Ahmed *et al.*, "Computer vision and photosensor based hybrid control strategy for a two-axis solar tracker - Daylighting application," *Solar Energy*, vol. 224, pp. 175–183, Aug. 2021, doi: 10.1016/j.solener.2021.05.077.

[21] C. Jamroen, C. Fongkerd, W. Krongpha, P. Komkum, A. Pirayawaraporn, and N. Chindakham, "A novel UV sensor-based dual-axis solar tracking system: Implementation and performance analysis," *Applied Energy*, vol. 299, pp. 1-17, Oct. 2021, doi: 10.1016/j.apenergy.2021.117295.

[22] J. Sigut, M. Castro, R. Arnay, and M. Sigut, "OpenCV Basics: A Mobile Application to Support the Teaching of Computer Vision Concepts," *IEEE Transactions on Education*, vol. 63, no. 4, pp. 328–335, Nov. 2020, doi: 10.1109/TE.2020.2993013.

[23] E. Cervera, "GPU-Accelerated Vision for Robots: Improving System Throughput Using OpenCV and CUDA," *IEEE Robot Autom Mag*, vol. 27, no. 2, pp. 151–158, Jun. 2020, doi: 10.1109/MRA.2020.2977601.

[24] X. Liu, M. Li, B. Li, and B. Fan, "Membrane–Fresnel Diffractive Lenses with High-Optical Quality and High-Thermal Stability," *Polymers (Basel)*, vol. 14, no. 15, pp. 1-11, Jul. 2022, doi: 10.3390/polym14153056.

[25] B.-Y. Huang, T.-H. Chen, T.-Y. Chen, J.-D. Lin, T.-H. Lin, and C.-T. Kuo, "A Planar Fresnel Lens in Reflection Type Based on Azo-Dye-Doped Cholesteric Liquid Crystals Fabricated by Photo-Alignment," *Polymers (Basel)*, vol. 12, no. 12, pp. 1-8, Dec. 2020, doi: 10.3390/polym12122972.

[26] M. Gupta, A. K. Dubey, V. Kumar, and D. S. Mehta, "Experimental study of combined transparent solar panel and large Fresnel lens concentrator based hybrid PV/thermal sunlight harvesting system," *Energy for Sustainable Development*, vol. 63, pp. 33–40, Aug. 2021, doi: 10.1016/j.esd.2021.05.008.

BIOGRAPHIES OF AUTHORS

Muhammad Ghozi Witsqa Ramadhan received Bachelor of Engineering (B.Eng.)/Sarjana Teknik (S.T.) degree in Electrical Engineering (Mechatronics Major) from Parahyangan Catholic University (UNPAR), Indonesia, in 2024. He can be contacted at email: muhammadghozi343@gmail.com.

Levin Halim completed his undergraduate studies in electrical power engineering and postgraduate studies in electrical engineering at the Bandung Institute of Technology in Indonesia in 2014 and 2015, respectively. Currently, he is responsible for being an assistant professor in the Department of Electrical Engineering at Parahyangan Catholic University. The research area includes renewable energy, power quality, power electronics, power generation, power delivery, power supply quality, power transmission reliability, power transmission lines, power transmission planning, power transmission protection, battery chargers, circuit breakers, harmonic distortion, load flow control, power distribution protection, and the use of artificial intelligence in power systems. He can be contacted at email: halimlevin@unpar.ac.id.

Faisal Wahab is a lecturer at the Parahyangan Catholic University in the Electrical Engineering Study Program with a concentration in Mechatronics. He obtained his bachelor's degree at the Indonesia University of Education in Electrical Engineering Education (2011) and a master's degree from the Bandung Institute of Technology in the School of Electrical and Informatics Engineering (2015). His interests and expertise include the fields of robotics, system modeling, electronics, and intelligent control systems. He can be contacted at email: faisal.wahab@unpar.ac.id.